第32卷第12期 焊 接 学 报 Vol. 32 No. 12
2011年12月 TRANSACTIONS OF THE CHINA WELDING INSTITUTION December 2011

钛合金表面氩弧熔覆原位合成 TiB_2–TiN 涂层组织及耐磨性能

王振廷， 丁元柱， 梁 刚
（黑龙江科技学院 材料科学与工程学院，哈尔滨 150027）

王振廷

摘 要： 以BN和Ni60A合金粉末为熔覆材料，采用氩弧熔覆技术在TC4合金表面原位合成 TiB_2–TiN 增强颗粒耐磨涂层. 利用X射线衍射仪、扫描电子显微镜和摩擦磨损试验机对熔覆层的组织和性能进行分析测试. 结果表明，复合涂层的显微组织沿层深方向分为熔覆区、结合区和热影响区；熔覆层与基体呈良好冶金结合，TiB_2–TiN 颗粒弥散分布，尺寸细小；涂层具有较高的硬度，在室温干滑动磨损试验条件下具有优良的耐磨性能；其磨损机制为显微切削磨损和粘着磨损.

关键词： 氩弧熔覆； 原位合成； 二硼化钛和氮化钛颗粒； 耐磨性
中图分类号： TG174.44 **文献标识码：** A **文章编号：** 0253－360X(2011)12－0105－04

0 序 言

钛合金具有比强度高、耐蚀性能好等优点，是航空航天、石油化工等领域广泛使用的理想材料. 但由于钛合金的摩擦系数较大，耐磨性和导热性能差，当用在机械工程中的摩擦部位时，易产生磨损而造成零部件失效，因此限制钛合金在工程领域应用[1,2]. 研究人员采用气相沉积、离子注入、激光熔覆等表面改性方法来提高钛合金的耐磨性能取得了积极进展. 在金属材料表面制备金属基陶瓷涂层，将金属材料的强韧性和陶瓷材料的耐磨耐蚀等性能结合起来是目前研究人员关注的技术热点[3－5]. 复合涂层中的陶瓷颗粒可以通过“外加法”获得，也可以通过在某种热源的条件下元素之间发生化学反应原位合成. 由于原位合成法制备金属基复合材料具有基体与增强相的相容性好，界面洁净，与基体冶金结合等优点，目前已受到了国内外研究人员的普遍关注[6－8]. 文中以BN和Ni60A合金粉末为熔覆材料，采用氩弧熔覆技术在TC4合金表面原位合成 TiB_2–TiN 增强颗粒耐磨涂层，对涂层的显微组织和耐磨性能进行了分析研究.

1 试验方法

基体材料选用TC4合金，试样尺寸为50 mm×10 mm×10 mm. 熔覆材料选用平均粒度为10 μm的Ni60A自熔合金粉末和平均粒度为20 μm的BN粉末，设计了质量分数为40% BN + 60% Ni60A（试样 S_1）、30% BN + 70% Ni60A（试样 S_2）和20% BN + 80% Ni60A（试样 S_3）合金粉末熔覆材料组分. 将BN粉和Ni60A粉混合搅拌均匀，用粘结剂将其调成糊状并密实涂覆在TC4合金基底试样表面，预置厚度为1.2 mm，放置通风处自然干燥12 h后置入干燥箱中，加热至90 ℃保温2 h，保证涂覆层具有较高的强度.

氩弧熔覆试验采用MW3000型数字焊接机，工艺参数为：熔覆电流110 A，熔覆速度8 mm/s，氩气流量14 L/min. 熔覆后降至室温，经磨光、抛光制备金相试样，用体积比为5∶5∶90的 HNO_3–HF–H_2O 腐蚀剂进行腐蚀，时间为1 min左右.

利用D/max–RB12型X射线衍射仪进行涂层的物相分析，MX–2600FE扫描电子显微镜观察分析微观组织和试样磨损形貌. 利用MHV2000型显微硬度仪测量氩弧熔覆试样涂层沿熔深方向的显微硬度（载荷1.96 N，加载时间10 s）. 室温干滑动磨损试验在MMS–2A摩擦磨损试验机上进行，采用环–块滑动干摩擦方式进行耐磨性能测试，试样尺寸10 mm×10 mm×6 mm，对磨环为GCr15的圆环试样，硬度63～66 HRC，试验参数为：旋转速率200 r/min，载荷200 N，时间120 min. 利用精度为0.000 1 g的FC204型电子天平称量试样的磨损量.

收稿日期：2010－09－30

2 试验结果与分析

2.1 复合涂层组织的物相分析

图 1 为氩弧熔覆原位生成 TiB_2-TiN 复合涂层的 X 射线衍射图谱. 通过对 X 射线图谱的分析标定可知，复合涂层的主要组成相为 TiB_2，TiN 和 Ti(Ni,Cr) 固溶体. 图 2 为氩弧熔覆涂层组织 SEM 形貌. 涂层均匀，无气孔、裂纹缺陷. 涂层分为熔覆区、结合区和热影响区. TiN 呈块状颗粒，TiB_2 呈针状分布在熔覆区.

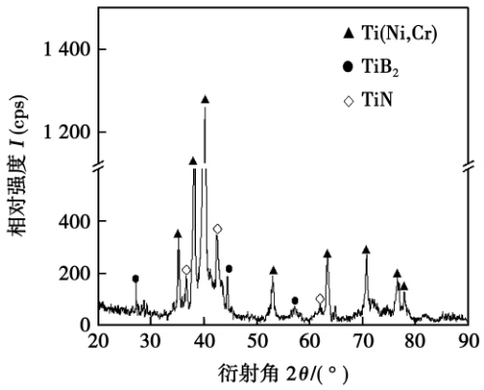

图 1 氩弧熔覆涂层 X 射线衍射图谱

Fig. 1 XRD pattern of composite coating surface

2.2 氩弧熔覆 TiB_2-TiN 复合涂层的硬度分布

图 3 为三种成分配比试样 S_1，S_2 和 S_3 的氩弧熔覆涂层的硬度分布曲线. 由图 3 可见，复合涂层具有较高的硬度，最高可达 1 250 HV. 不同成分配比的复合涂层显微硬度曲线呈现大致相同的趋势走向，随着 BN 粉含量的增加，原位合成的增强相颗粒体积分数增大，复合涂层的显微硬度随之提高，增强效果更加明显. 分析认为，氩弧作为热源使 TC4 合金和 BN 粉熔化形成了大量的高强度、高硬度的 TiB_2 和 TiN 硬质颗粒，弥散分布在基体的表面上(图 2)，这样使得基体表层硬度得到了提高.

2.3 氩弧熔覆 TiB_2-TiN 复合涂层的耐磨性能

图 4 为三种成分配比 S_1，S_2，S_3 试样氩弧熔覆复合涂层和钛合金 TC4 在相同摩擦工作参数(滑动时间 $t = 120$ min，法向载荷 $F = 200$ N，滑动速度 $v = 200$ r/min) 下的磨损失重量. 可以看出，复合涂层的磨损失重量随熔覆材料 BN 粉末量的减少而增加，试样 S_1(40% BN + 60% Ni60A) 的复合涂层磨损失重量最小，S_2，S_3 磨损失重量有所增加，TC4 的磨损失重量最大，大约分别是 S_1，S_2，S_3 磨损失重量的 16 倍、5 倍和 2 倍，因而试样 S_1 复合涂层具有较好的

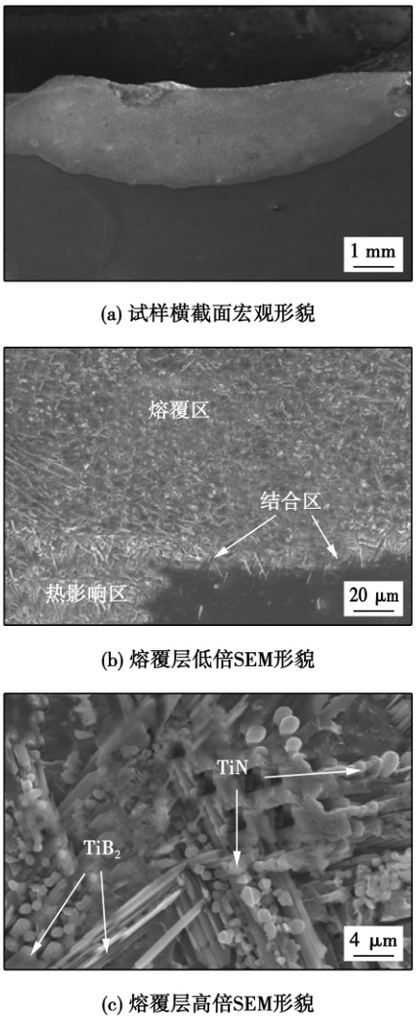

图 2 氩弧熔覆涂层组织 SEM 形貌

Fig. 2 SEM micrographs of composite coating

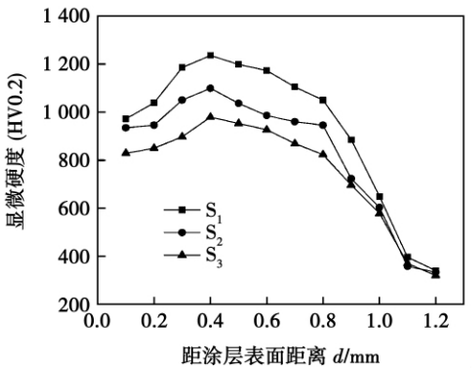

图 3 复合涂层沿层深方向显微硬度分布曲线

Fig. 3 Microhardness of composite coating

耐磨性能. 原因是由于 BN 质量分数的增加，生成的陶瓷增强相 TiB_2 和 TiN 颗粒增多，弥散分布于基体中，覆盖了合金表面带棱角的质点，在基体表面形成了一层覆盖层，TiB_2 的显微硬度为 34 GPa，TiN 的硬

度约为 20 GPa，TiN 的生成自由能低，物理化学性能稳定，因此 TiN 在磨损试验时表现出良好的硬度和抗磨性，TiN 和 TiB_2 的共同作用使得涂层显示出优良的耐磨性.

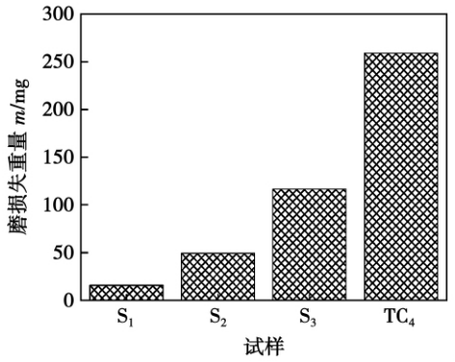

图 4　复合涂层和 TC4 的磨损失重对比图

Fig. 4　Wear loss comparison of composite coatings and TC4 alloy

图 5 为 TC4 合金和 S_1 试样的磨损表面形貌. 由图 5a 看出，在 TC4 合金试样表面明显可以看出沿滑动方向的划痕，上面残留细小的磨屑，划痕是由于磨屑和 GCr15 钢中的硬质点对 TC4 合金试样的磨粒切削作用造成的. 同时在 GCr15 钢和 TC4 合金试样表面存在材料“粘附转移”现象，这表明与之对磨的材料发生了粘着磨损. 因此，TC4 合金的磨损机制主要为磨粒磨损和粘着磨损. 图 5b 为复合涂层背散射图像，由于磨损产生的磨屑非常少，因此在图中看不见基体产生明显的犁沟，只能看到涂层基体表面沿摩擦滑动方向分布着数量较少且不连续的磨痕，并且在增强相 TiB_2 和 TiN 颗粒表面也看不到明显的划痕，如同磨痕从颗粒表面“越”过去，终止于颗粒前沿，开始于颗粒后端，没有对增强相造成严重的切削和划伤，因此未见颗粒脱落迹象. 这可能是由于复合涂层增强相体积分数大，分布数量较多，其抗磨支撑作用使得磨损难以向涂层深处进行. 因此对涂层造成显微切削磨损.

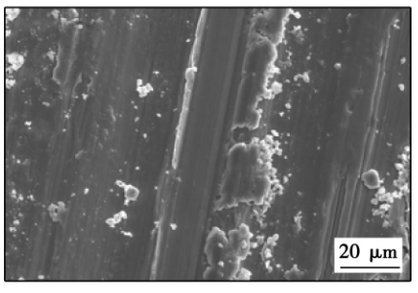

(a) TC4合金磨损表面形貌

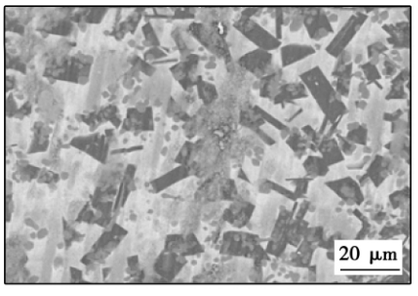

(b) S_1试样背散射磨损表面形貌

图 5　TC4 合金和 S_1 试样背散射磨损表面形貌

Fig. 5　Wear surface morphology of TC4 alloy and composite coating of S_1 BEI

试验过程（室温干滑动磨损试验，对磨环为 GCr15 的圆环试样，硬度 63 ~ 66 HRC，试验参数为旋转频率 200 r/min，载荷 200 N，时间 120 min）中发现，当复合涂层与 GCr15 钢试样摩擦磨损达到一定程度后，GCr15 钢试样表面氧化. 由于复合涂层的硬度较高，GCr15 钢表面的磨损较为严重，其表面磨损速率大于表面氧化膜形成的速率. 随着磨损过程的进行，试样表面温度提高，逐渐的磨掉氧化膜层，GCr15 钢表面就会不断地露出新生的金属表面，增大了与复合涂层表面粘着的倾向. 对 TC4 合金表面金属转移物进行能谱分析，其成分（质量分数，%）约为 C 3.0，O 34.70，Si 0.62，Ti 7.52，Fe 51.37，Cr 1.97，Ni 0.82，可以看出这些转移物的主要成分是铁的氧化物，来自于对磨副 GCr15 钢，说明在磨损过程中发生了粘着磨损. 因此，氩弧熔覆复合涂层的磨损机制主要为显微切削磨损和粘着磨损.

3　结　　论

（1）适宜的氩弧熔覆工艺参数下，在 TC4 表面熔覆 BN 和 Ni60A 合金粉末可以原位反应生成 TiB_2-TiN 增强颗粒复合陶瓷涂层. 显微组织沿层深方向分为熔覆区、结合区和热影响区三个区域.

（2）随着 BN 粉含量的增加，增强相 TiB_2 和 TiN 颗粒增多，复合涂层的显微硬度和耐磨性提高. 试样 S_1（40% BN + 60% Ni60A）显微硬度最高可达 1 250 HV，具有优良的耐磨性能.

（3）TC4 合金的磨损机制主要为磨粒磨损和粘着磨损，氩弧熔覆复合涂层的磨损机制主要为显微切削磨损和粘着磨损.

参考文献：

[1]　张喜燕，赵永庆，白晨光. 钛合金及应用 [M]. 北京：化学工

业出版社，2005.

[2] 张嗣伟. 我国摩擦学工业应用的节约潜力巨大 [J]. 中国表面工程，2008，21(2)：50－52.
Zhang Siwei. Enormous economy potential of tribology application in industry in china [J]. China Surface Engineering，2008，21(2)：50－52.

[3] Tjong S C，Ma Z Y. Microstructure and mechanical characteristics of in situ metal matrix composites [J]. Materials Science and Engineering，2000，29：49－113.

[4] Maity Y P C，Panigrshi S C. Metal and intermetallic matrix in situ particle composites [J]. Key Engineering Materials，1995，108/110：313－328.

[5] Srivatsan T S. Tensile deformation and fracture behavior of a titanium-alloy metal-matrix composite [J]. Composites Part A，1997，28A：365－376.

[6] 肖代红，黄伯云. 原位合成钛基复合材料的最新进展 [J]. 粉末冶金技术，2008，26(3)：217－223.
Xiao Daihong，Huang Boyun. New progress on in situ titanium matrix composites [J]. Powder Metallurgy Technology，2008，26(3)：217－223.

[7] 宋思利. 钨极氩弧原位合成 TiC 增强铁基熔敷层的研究 [D]. 山东大学，2007.

[8] 王振廷，陈丽丽，张显友. 钛合金表面氩弧熔覆 TiC 增强复合涂层组织与性能分析 [J]. 焊接学报，2008，29(9)：43－45.
Wang Zhenting，Chen Lili，Zhang Xianyou. Microstructure and properties of TIC reinforced composite coating fabricated on Ti alloy by GTAW [J]. Transactions of the China Welding Institution，2008，29(9)：43－45.

作者简介： 王振廷，男，1965 年出生，博士后，教授. 主要从事耐磨材料和材料表面工程方面的教学和科研工作. 发表论文 40 余篇. Email：wangzt2002@163.com

[上接第 72 页]

粗大，热影响区范围比较大. 金相的变化说明超声振动的能量成功地注入到焊缝的底部，金属组织有较为明显的晶粒细化和组织均匀化的积极效果，加入超声振动能有效地改善金属的塑性流动状态，改善焊缝效果.

3 结 论

(1) 提出了超声搅拌复合焊的新方法，在对 2219 铝合金的试验中尝试将超声波通过搅拌针导入焊缝底部，以减少变形阻力和流动应力，提高焊缝底部材料的流动性能，获得高质量焊缝.

(2) 2219 铝合金超声搅拌焊接试验效果非常明显，超声的导入使得晶粒更加细小，组织分布更均匀，材料的流动性有很明显的改善.

(3) 超声搅拌焊得到的铝合金焊缝抗拉强度大大提高，显微组织更致密更均匀，证实了超声搅拌复合焊接能够对铝合金焊接过程产生积极改善效果，用超声搅拌复合焊接改善材料焊缝底部组织的思路是可行的.

参考文献：

[1] 张 华，林三宝，吴 林，等. 搅拌摩擦焊研究进展及前景展望 [J]. 焊接学报，2003，24(3)：91－96.
Zhang Hua，Lin Sanbao，Wu Lin. *et al*. Progress and prospects of friction stir welding [J]. Transactions of the China Welding Institution，2003，24(3)：91－96.

[2] 周鹏展，钟 掘，贺地求，等. 2519 厚板搅拌摩擦焊接工艺组织分析 [J]. 中南大学学报，2006，37(4)：114 － 118.
Zhou Pengzhan，Zhong Jue，He Diqiu. *et al*. Organization analysis of 2519 thick plate friction stir welding process [J]. Centre South University Journal，2006，37(4)：114－118.

[3] 周鹏展，李东辉，贺地求，等. 2219-T6 厚板搅拌摩擦焊沿厚度方向的性能差异 [J]. 焊接学报，2007，28(10)：5－8.
Zhou Pengzhan，Li Donghui，He Diqiu，*et al*. The performance difference along the thickness direction of 2219-T6 friction stir welding [J]. Transactions of the China Welding Institution，2007，28(10)：5－8.

[4] 金长善. 超声加工 [M]. 哈尔滨：哈尔滨工业大学出版社，1989.

[5] 何 勍，闻邦春. 振动塑性加工的进展及若干问题 [J]. 辽宁工学院学报，1999，19(4)：8－10.
He Qiong，Wen Bangchun. Progress and many issues of vibrations plastic processing [J]. Journal of Liaoning Institute，1999，19(4)：8－10.

[6] Yang S Q，Dang Z，Yah J C，*et al*. Simulation on heating process in ultrasonic welding of plastics [J]. Acta Allurgica Sinica，2000，13(1)：80－83.

[7] Devine J. Ultrasonic plastics welding basics [J]. Welding Joumal，2001，80(3)：29－33.

[8] Eskin G I. Ultrasonic treatment of light alloy melts [M]. Amsterdam：Gordon & Breach，1998.

[9] Abramov O V. Action of high intensity ultrasonic on solidifying metal [J]. Ultrasonic，1987，25(2)：73－82.

作者简介： 贺地求，男，1963 年出生，硕士，教授. 主要从事厚板搅拌摩擦焊接工艺及机理研究. 发表论文 20 余篇. Email：wc3lijian@126.com

HUANG Wenrong, MO Zhonghai (Institute of Machinery Manufacturing Technology, China Academy of Engineering Physics, Mianyang 621900, China). p 93 - 96, 100

Abstract: Experimental investigations on the electron beam welding of aluminum alloy 2A14 are presented in this paper. Experiments are carried out to study the influence of welding parameters, such as beam current, welding speed, focal location, scanning graph, graph size and scanning frequency, on the penetration depth and width of welds based on an orthogonal test and analysis method. The results showed beam current and focal location had the greatest effect on penetration depth and width of welds, welding speed was next, and beam scanning parameters, such as figures, size and frequency, relatively affected much less. The joints welded by the optimum parameters are good appearance and quality. The microstructure of weld zone is composed of α phase and eutectic structure grains.

Key words: electron beam welding; aluminum alloy; orthogonal test and analysis; microstructure

Study of friction-stir-welded lap joint of aluminum and zinc-coated steel WANG Xijing, SHEN Zhikang, ZHANG Zhongke (State Key Laboratory of Advanced New Non-ferrous Materials, Lanzhou University of Technology, Lanzhou 730050, China). p 97 - 100

Abstract: Lap joint friction stir welding of dissimilar materials between DP600 dual-phase zinc-coated steel and industrial pure aluminum 1060 (the aluminum plate was on the top and the steel was under it) was researched in this paper. It can be found from microstructure morphology of the joint that the steel inserts the aluminum just like two nails in both the advancing side and return side. On the micro scale, the steel and aluminum fully mixed together like rivers. In the weld, nugget zone and heat affected zone, a layer of a certain width of the transition layer was formed by the two materials staggered together. Mechanical performance tests show that the hardness of transition layer is high, joint shear strength is about 77% of base metal, and the mechanical properties of the weld is good. Intermetallic compound $Al_{13}Fe_4$ is found on the fractured surface through XRD phase analysis.

Key words: friction stir welding; aluminum plate; zinc-coated steel; mechanical properties; intermetallic compound

Electric and thermal characteristics of micro-plasma torch LIU Gu[1], WANG Liuying[1,2], CHEN Guiming[1], YUAN Yuhua[3], WEI Wanning[1] (1. The 5th Staff of Second Artillery Engineering College, Xi'an 710025, China; 2. Key Laboratory of Electronic Ceramics and Devices of Ministry of Education, Xi'an Jiaotong University, Xi'an 710049, China; 3. Equipment Institute of the Second Artillery, Bejing 100085, China). p 101 - 104

Abstract: The voltage-current characteristic and thermal efficiency of a plasma gun are key factors influencing the quality of the plasma spraying process. The electric and thermal characteristics of the newly developed micro-plasma torch were investigated. As one of the factors effecting the plasma arc voltage, gas injection was also researched in this paper. The plasma arc voltage for the radial injection mode is much lower than that of axial injection mode and the integrated mode. However, the current-voltage characteristics of the plasma jet show a decreasing tendency in spite of the three gas injection modes. With the integrated mode, stable and long plasma jet with high heat energy was obtained. The thermal efficiency of the micro-plasma gun ranges from 56% to 76%, and the plasma enthalpy is 3.28 kJ/g ~ 11.16 kJ/g. With designed special plasma gun structure and integrated gas injection mode, the plasma gun shows a high thermal efficiency and plasma enthalpy which is suitable for the coating preparation with high qualities.

Key words: micro-plasma; gas injection mode; voltage-current characteristic; thermal efficiency

Microstructure and wear resistance of in-situ synthesis TiB_2-TiN particulates of composite coating reinforced titanium alloy surface by argon arc cladding WANG Zhenting, DING Yuanzhu, LIANG Gang (College of Materials Science and Engineering, Heilongjiang Institute of Science and Technology, Harbin 150027, China). p 105 - 108

Abstract: The composite coating reinforced by in-situ synthesized TiB_2 and TiN particulates was prepared on the surface of TC4 alloy by means of argon arc cladding using BN and Ni60A powders as raw materials. The microstructure of TiB_2-TiN composite coating were characterized by means of X-ray diffraction (XRD) and scanning electron microscopy (SEM). The wear properties of coating were examined using friction and wear tester. Experimental results show that three regions with different microstructures existed in the coating, the cladding zone, the binding zone and the heat-affected zone along the depth profile. There is a good metallurgical bonding between the composite coating and the substrate, the TiB_2 and TiN particulates are dispersively distributed in the coating. The composite coating exhibits high microhardness and excellent wear resistance under dry sliding wear test condition. The wear mechanism of the coating is micro-cutting wear and adhesive wear.

Key words: argon arc cladding; in-situ synthesis; TiB_2 and TiN particulates; wear resistance

Effect of CeO_2 on microstructure and properties of Fe-based coating produced by plasma arc cladding process LI Diankai[1], LI Mingxi[1], HONG Haifeng[1], GAO Huhe[2], WANG Guilin[2] (1. School of Materials Science & Engineering, Anhui Key Lab of Metal Material and Processing, Anhui University of Technology, Ma'anshan 243002, China; 2. Anhui Taier Heavy Industry Co., Ltd., Ma'anshan 243000, China). p 109 - 112

Abstract: The effect of addition of 1% CeO_2 on the microstructure and wear resistance of high chromium cast iron coating produced by plasma arc cladding process was investigated by means of optical microscope (OM), scanning electron microscope (SEM), X-rays diffraction (XRD) and sliding wear testing. The results show that the phases composition of the alloy coating compared with the Fe-iron coating was not changed, both consisted of γ-(Ni, Fe) solid solution with a face-centered cubic lattice and M_7C_3 (M = Cr, Fe, Mo) carbides with a hexagonal structure. Heterogeneous nucleation of the alloy coating modified with rare earth oxide CeO_2 that leads to the microstructure refinement and restrains the growth of carbides. And it changes the crystal growth direction of γ-(Fe, Ni) solid solution from both {111} and {002} to single {002}. Meanwhile, the rare earth oxides homogeneously distribute in eutectic microstructure, thus improving the microhardness and wear resistance of the coating.

Key words: plasma arc cladding; Fe-based alloy; rare earth oxides; wear resistance